Supporting Information

Particularly strong C-H···π interactions between benzene and all-*cis*1,2,3,4,5,6-hexafluorocyclohexane

Rodrigo A. Cormanich,[a,b] Neil S. Keddie,[a] Roberto Rittner,[b] David O'Hagan[a] and Michael Bühl,[a*]

[a] *EastChem School of Chemistry, University of St Andrews, North Haugh, St Andrews, Fife, KY16 9ST, UK*

[b] *Chemistry Institute, State University of Campinas, P.O. Box 6154, 13083-970, Campinas, SP, Brazil*

E-mail: mb105@st-andrews.ac.uk

Computational details

Geometries were fully optimized at the B3LYP/def2-TZVP, B3LYP-D3/def2-TZVP and MP2/aug-cc-pVDZ levels, and magnetic shieldings evaluated at the BHandH/6-311+G(2d,p) level for each geometry by using the Gaussian 09 Revision D.01 program.[1] DFT calculations employed a fine integration grid (i.e. 75 radial shells with 302 angular points per shell). At that level, the B3LYP optimised structure displayed a small imaginary frequency ($3i$ cm^{-1}), which vanished upon reoptimisation with tighter optimisation thresholds and an ultrafine integration grid (i.e. 99 radial shells with 590 angular points per shell). Optimisations for the complexes with benzene were performed including correction for basis-set superposition error (BSSE) by way of the Counterpoise method.[2] ^{1}H magnetic shieldings were converted into relative chemical shifts δ using the ^{1}H magnetic shielding in TMS computed at the same respective levels. The energies were converted into enthalpies and Gibbs free energies using standard thermodynamic corrections from the frequency calculations for each level.Complete basis set calculations were performed using the extrapolation scheme by Helgaker and coworkers.[3] This procedure is based on calculations with Dunning's correlation-consistent basis sets[4] with increasing cardinal numbers and involves separate extrapolation for HF and the second-order perturbation correction $E^{(2)}$, using inverse exponential and cubic fits, respectively. We did this for the calculated absolute energies (not corrected for BSSE) from MP2 (and SCS-MP2)/aug-cc-pVxZ single points (x = D, T, Q) on MP2/aug-cc-pVDZ optimised geometries (HF single points up to aug-cc-pV5Z basis). Extrapolations of energies obtained including Counterpoise corrections or using an inverse quadratic fit for $E^{(2)}$ afforded very similar CBS limits for each system, all within ca. ±0.4 kcal/mol of the "standard" fit (slightly larger variations up to ±0.6 kcal/mol were obtained when both BSSE corrections and an inverse quadratic fit were used, see Tables S2-S5 for details and results). When complexation energies rather than absolute energies were extrapolated, similar standard deviations were obtained from the fitting procedure (±0.4 kcal/mol, Table S3). Because these fits of complexation energies do not

1 Gaussian 09, Revision D.01, M. J. Frisch, G. W. Trucks, H. B. Schlegel, G. E. Scuseria, M. A. Robb, J. R. Cheeseman, G. Scalmani, V. Barone, B. Mennucci, G. A. Petersson, H. Nakatsuji, M. Caricato, X. Li, H. P. Hratchian, A. F. Izmaylov, J. Bloino, G. Zheng, J. L. Sonnenberg, M. Hada, M. Ehara, K. Toyota, R. Fukuda, J. Hasegawa, M. Ishida, T. Nakajima, Y. Honda, O. Kitao, H. Nakai, T. Vreven, J. A. Montgomery, Jr., J. E. Peralta, F. Ogliaro, M. Bearpark, J. J. Heyd, E. Brothers, K. N. Kudin, V. N. Staroverov, R. Kobayashi, J. Normand, K. Raghavachari, A. Rendell, J. C. Burant, S. S. Iyengar, J. Tomasi, M. Cossi, N. Rega, J. M. Millam, M. Klene, J. E. Knox, J. B. Cross, V. Bakken, C. Adamo, J. Jaramillo, R. Gomperts, R. E. Stratmann, O. Yazyev, A. J. Austin, R. Cammi, C. Pomelli, J. W. Ochterski, R. L. Martin, K. Morokuma, V. G. Zakrzewski, G. A. Voth, P. Salvador, J. J. Dannenberg, S. Dapprich, A. D. Daniels, Ö. Farkas, J. B. Foresman, J. V. Ortiz, J. Cioslowski, and D. J. Fox, Gaussian, Inc., Wallingford CT, **2009**.

2 (a) S. F. Boys, F. Bernardi *Mol. Phys.* 1970, **19**, 553. (b) S. Simon, M. Duran, J. J. Dannenberg, *J. Chem. Phys.* 1996, *105*, 11024.

3 T. Helgaker, W. Klopper, H. Koch, J. Noga, *J. Chem. Phys.* 1997, **106**, 9639.

4 (a) T. H. Dunning Jr., *J. Chem. Phys.*, 1989, **90**, 1007. (b) R. A. Kendall, T. H. Dunning Jr., R. J. Harrison, *J. Chem. Phys.*, 1992, **96**, 6796. (c) D. E. Woon, T. H. Dunning Jr., *J. Chem. Phys.* 1993, **98**, 1358. (d) K. A. Peterson, D. E. Woon, T. H. Dunning Jr., *J. Chem. Phys.*, 1994, 100, 7410. (e) A. K. Wilson, T. van Mourik, T. H. Dunning Jr., *J. Mol. Struct. (Theochem)*, 1996, **388**, 339.

show the proper convergence behavior of those using absolute energies (Figure S1), we used only the latter (for which the basis sets were designed). We report the "standard" fit results according to Helgaker et al[3] (i.e. without Counterpoise correction and using an inverse cubic fit) and use the ±0.4 kcal/mol variation as a conservative error estimate.

The MP2/aug-cc-pVDZ total electron densitiy was evaluated for the geometry of $\mathbf{3}^{.}C_6H_6$ optimised at that level (optimisation done including Counterpoise correction) and was used to run QTAIM (quantum theory of atoms in molecules)[5] and NCI (non-covalent interactions) calculations[6] using the AIMALL[7] and NCIPLOT 3.0 programs,[6] respectively.

Experimental Details

All cis-1,2,3,4,5,6-hexafluorocyclohexane was synthesised in 12-steps, as a colourless solid (cf. reference 4 of the main paper): mp 206–208 ˚C (CH_2Cl_2); ^{1}H NMR (700 MHz, CD_2Cl_2) δ_H 5.40-5.23 (3H, m, H_{eq}) and 4.61-4.46 (2H, m, H_{ax}); ^{13}C NMR (125 MHz, CD_2Cl_2) δ_C 89.5-84.3 (6C, m).

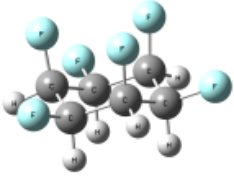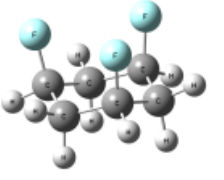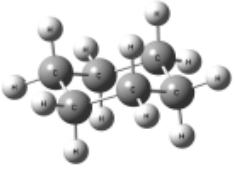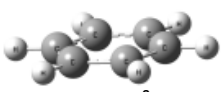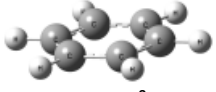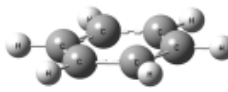Melting points were determined on a Reichert hot stage microscope and are uncorrected.

^{1}H NMR measurements were carried out on a Bruker Avance III 700 spectrometer, equipped with a TXI probe, operating at 700 MHz, using the deuterated solvent as the reference for internal deuterium lock. ^{13}C NMR measurements were carried out on a Bruker Avance III HD spectrometer, equipped with a BBFO probe, operating at 125 MHz with broadband ^{1}H decoupling, using the deuterated solvent as the reference for internal deuterium lock. The chemical shift data are given as δ in units of parts per million (ppm) relative to tetramethylsilane (TMS) where δ (TMS) = 0.00 ppm. Each spectrum was referenced to the residual solvent signal. The solutions for NMR analysis were prepared by mixing hexafluorocyclohexane with d_2-dichloromethane (CD_2Cl_2) or d_6-benzene (C_6D_6) and sonicating the mixture for 30 s. Any remaining solids were allowed to settle, before the solution was decanted to a 5 mm NMR tube. The final concentration of the solutions was estimated to be ≤ 1 mgmL^{-1}.

5 R. F. W. Bader, *Atoms in Molecules: A Quantum Theory*, Clarendon, Oxford, 1990.

6 E. Johnson, S. Keinan, P. Mori-Sánchez, J. Contreras-García, A. Cohen, W. Yang, *J. Am. Chem. Soc.*, 2010, **132**, 6498.

7 AIMAll (Version 14.11.23), T. A. Keith, TK Gristmill Software, Overland Park KS, USA, 2013 (aim.tkgristmill.com).

Table S1: Distances between the benzene ring and the cyclohexane axial hydrogen atoms C-H···π (angstroms) and binding energies (kcal mol^{-1}) for raw potential energies (ΔE), enthalpies (ΔH) and Gibbs free energies (ΔG) for compounds **3-5**.

		3	**4**	**5**
B3LYP	**C-H···π**	3.105 Å	3.442 Å	---
	ΔE	-2.12	-0.75	---
	ΔH	-1.30	-0.04	---
	ΔG	+6.12	+6.98	---
B3LYP-D3	**C-H···π**	2.694 Å	2.786 Å	2.834 Å
	ΔE	-7.06	-4.84	-3.40
	ΔH	-6.80	-4.71	-2.63
	ΔG	+4.63	+5.92	+5.27
MP2[a]	**C-H···π**	2.710 Å	2.805 Å	2.868 Å
	ΔE	-6.95	-4.88	-3.17
	ΔH	-6.13	-4.17	-2.40
	ΔG	+1.28	+2.85	+5.50

[a] MP2 thermal corrections were obtained from B3LYP-D3/def2-TZVP frequencies calculated from B3LYP-D3/def2-TZVP equilibrium geometry.

Table S2: Compounds **3** and **4** binding energies (kcal mol^{-1}) and C-H···π distances (angstroms) obtained at different levels.

	3				**4**			
	C-H···π	ΔE	ΔH[c]	ΔG[c]	C-H···π	ΔE	ΔH[c]	ΔG[c]
Optimisations[a]								
B3LYP/def2-TZVP	3.105	-2.12	-1.30	+6.12	3.442	-0.75	-0.04	+6.98
B3LYP-D3/def2-TZVP	2.694	-7.06	-6.80	+4.63	2.786	-4.84	-4.71	+5.92
HF/aug-cc-pVDZ	3.321	-2.55	-2.32	+7.30	3.672	-1.04	-0.92	+7.22
MP2/aug-cc-pVDZ	2.710	-6.95	-6.13	+1.28	2.805	-4.88	-4.17	+2.85
Single points[b]								
HF/aug-cc-pVDZ	2.710	-2.31	-2.09	+7.54	2.805	-0.09	+0.02	+8.16
HF/aug-cc-pVTZ	2.710	-0.55	-0.32	+9.31	2.805	+1.15	+1.27	+9.41
HF/aug-cc-pVQZ	2.710	-0.22	+0.01	+9.63	2.805	+1.36	+1.47	+9.61
HF/aug-cc-pV5Z	2.710	-0.14	+0.08	+9.71	2.805	+1.40	+1.52	+9.66
MP2/aug-cc-pVDZ	2.710	-12.16	-11.33	-3.92	2.805	-8.96	-8.25	-1.23
MP2/aug-cc-pVTZ	2.710	-9.30	-8.48	-1.07	2.805	-6.82	-6.12	+0.90
MP2/aug-cc-pVQZ	2.710	-8.03	-7.21	+0.20	2.805	-5.78	-5.07	+1.95
SCS-MP2/aug-cc-pVDZ	2.710	-10.59	-9.77	+0.18	2.805	-7.55	-6.84	-2.35
SCS-MP2/aug-cc-pVTZ	2.710	-7.79	-6.97	+0.44	2.805	-5.44	-4.74	+2.28
SCS-MP2/aug-cc-pVQZ	2.710	-6.45	-5.63	+1.78	2.805	-4.33	-3.63	+3.39

[a] Optimisations with BSSE corrections included.

[b] Single point energy calculations on MP2/aug-cc-pVDZ optimised geometries.

[c] MP2 and SCS-MP2 levels used thermal corrections obtained from B3LYP-D3/def2-TZVP frequency calculations on B3LYP-D3/def2-TZVP geometries.

Table S3: Compounds **3** and **4** binding energies (kcal mol^{-1}) obtained with aug-cc-pVXZ basis sets (X = 2, 3 and 4; X = 5 for the HF method was also used). Complete basis set (CBS) energies were computed from the binding energies in kcal mol^{-1}.

	Compound 3	Compound 4
HF/CBS[a]	-0.13 +/- 0.009899	+1.41+/- +/- 0.002333
$E^{(2)}$/aug-cc-pVDZ	-9.85	-8.87
$E^{(2)}$/aug-cc-pVTZ	-8.75	-7.99
$E^{(2)}$/aug-cc-pVQZ	-7.81	-7.14
$E^{(2)}$/CBS[b]	-7.80 +/-0.3852	-7.16 +/-0.3643
$E^{(2)}$/CBS[c]	-7.36 +/- 0.3808	-6.79 +/- 0.3719
MP2/CBS[d]	-7.93 +/-0.395099	-5.75 +/-0.366633
$E^{(2)}$(SCS)/aug-cc-pVDZ	-8.28	-7.46
$E^{(2)}$(SCS)/aug-cc-pVTZ	-7.24	-6.59
$E^{(2)}$(SCS)/aug-cc-pVQZ	-6.23	-5.69
$E^{(2)}$(SCS)/CBS[b]	-6.26 +/- 0.4336	-5.73 +/- 0.3943
$E^{(2)}$(SCS)/CBS[c]	-5.81 +/- 0.4432	-5.35 +/- 0.4086
SCS-MP2/CBS[e]	-6.39 +/- 0.443499	-4.32 +/- 0.396633
SCS-MP2/CBS[f]	-5.94 +/- 0.453099	-3.94 +/- 0.410933

[a] Using the equation: E(HF) = a + be^{-cX} with X = 2, 3 ,4 and 5 from HF=aug-cc-pVXZ energies in Table X.
[b] Using the equation: $E^{(2)}$ = a + bX^{-3}.
[c] Using the equation: $E^{(2)}$ = a + bX^{-2}.
[d] MP2/CBS = HF/CBS + $E^{(2)}$/CBS
[e] SCS-MP2/CBS = HF/CBS + $E^{(2)}$(SCS)/CBS for the equation $E^{(2)}$ = a + bX^{-3}.
[f] SCS-MP2/CBS = HF/CBS + $E^{(2)}$(SCS)/CBS for the equation $E^{(2)}$ = a + bX^{-2}.

Table S4: Absolute energies (atomic units) for each monomer and complexes with benzene computed by using aug-cc-pVXZ basis sets (X = 2, 3 and 4; and X = 5 for the HF method). Complete basis set (CBS) extrapolated energies obtained from such energies and the fitting errors are indicated for each case.

		Benzene	pristine 3	pristine 4	3 C_6H_6	4 C_6H_6	3 C_6H_6 (BSSE)	4 C_6H_6 (BSSE)
HF	HF/aug-cc-pVDZ	-230.725567	-827.4090045	-530.8338317	-1058.13825964	-761.559549335	-1058.12996117	-761.55304855
	HF/aug-cc-pVTZ	-230.7767992	-827.6162631	-530.9635382	-1058.39393213	-761.738499213	-1058.39059527	-761.73584160
	HF/aug-cc-pVQZ	-230.7897778	-827.6693739	-530.9967429	-1058.45950072	-761.784358247	-1058.45840554	-761.78353054
	HF/aug-cc-pV5Z	-230.7925671	-827.68299	-531.0050983	-1058.47578529	-761.795427835	---	---
	HF/CBS	-230.793738	-827.68768	-531.00804	-1058.48164	-761.79955	-1058.48212	-761.80036
		+/- 0.0002799	+/- 3.564 x 10^{-6}	+/- 8.245 x 10^{-5}	+/- 0.0003018	+/- 0.0003871		
MP2	$E^{(2)}$/aug-cc-pVDZ	-0.8146531939	-2.053483824	-1.471268348	-2.883821808	-2.300043804	-2.87552333	-2.29354302
	$E^{(2)}$/aug-cc-pVTZ	-0.9662962696	-2.535339550	-1.797424260	-3.5155916010	-2.7764310120	-3.51225474	-2.77377340
	$E^{(2)}$/aug-cc-pVQZ	-1.018064346	-2.708096589	-1.910895023	-3.738608828	-2.940325405	-3.73751365	-2.93949769
	$E^{(2)}$/CBS[a]	-1.04081	-2.77802	-1.95921	-3.83128	-3.01141	-3.83077	-3.01101
		+/- 0.008511	+/- 0.03178	+/- 0.01952	+/- 0.03967	+/- 0.02746	+/- 0.04026	+/- 0.02797
	$E^{(2)}$/CBS[b]	-1.08641	-2.9246	-2.05772	-4.02275	-3.15493	-4.02385	-3.15579
		+/- 0.0008967	+/- 0.002818	+/- 0.0004691	+/- 0.001302	+/- 0.001949	+/- 0.001649	+/- 0.001617
SCS	$E^{(2)}$/aug-cc-pVDZ	-0.792957561	-1.987004461	-1.436611818	-2.793145931	-2.241449786	---	---
	$E^{(2)}$/aug-cc-pVTZ	-0.951338422	-2.4796638985	-1.7726714566	-3.442550322	-2.734523782	---	---
	$E^{(2)}$/aug-cc-pVQZ	-1.0082170037	-2.6675215692	-1.8965935015	-3.6856703568	-2.9138811635	---	---
	$E^{(2)}$/CBS[a]	-1.03117	-2.73585	-1.94439	-3.777	-2.98471	---	---
		+/- 0.0105	+/- 0.03892	+/- 0.02413	+/- 0.04872	+/- 0.03399		
	$E^{(2)}$/CBS[b]	-1.07937	-2.88799	-2.04732	-3.97664	-3.13522	---	---
		+/- 0.0009916	+/- 0.01058	+/- 0.004323	+/- 0.01086	+/- 0.004653		

[a] Using the equation: $E^{(2)} = a + bx^{-3}$.
[b] Using the equation: $E^{(2)} = a + bx^{-2}$.

Table S5: Binding energies (kcal mol^{-1}) obtained from CBS absolute energies showed in Table S4 for compounds **3** and **4**.

	3	4
HF/CBS	-0.13	+1.41
HF/CBS (BSSE)	-0.44	+0.89
$E^{(2)}$/CBS[a]	-7.81	-7.14
$E^{(2)}$/CBS[b]	-7.37	-6.78
$E^{(2)}$/CBS[a] (BSSE)	-7.49	-6.90
$E^{(2)}$/CBS[b] (BSSE)	-8.06	-7.32
MP2/CBS[c]	-7.93	-5.75
MP2/CBS[d]	-7.50	-5.37
MP2/CBS[c] (BSSE)	-7.62	-5.49
MP2/CBS[d] (BSSE)	-8.50	-6.43
$E^{(2)}$(SCS)/CBS[a]	-6.26	-5.74
$E^{(2)}$ (SCS)/CBS[b]	-5.82	-5.35
SCS-MP2/CBS[c]	-6.39	-4.33
SCS-MP2/CBS[d]	-5.95	-3.94

[a] $E^{(2)}$ = a + bX^{-3} from Table S4.
[b] $E^{(2)}$ = a + bX^{-2} from Table S4.
[c] MP2/CBS and SCS-MP2 = HF/CBS + $E^{(2)}$/CBS. $E^{(2)}$/CBS value used was that obtained from equation $E^{(2)}$ = a + bX^{-3}.
[d] MP2/CBS and SCS-MP2 = HF/CBS + $E^{(2)}$/CBS. $E^{(2)}$/CBS value used was that obtained from equation $E^{(2)}$ = a + bX^{-2}.

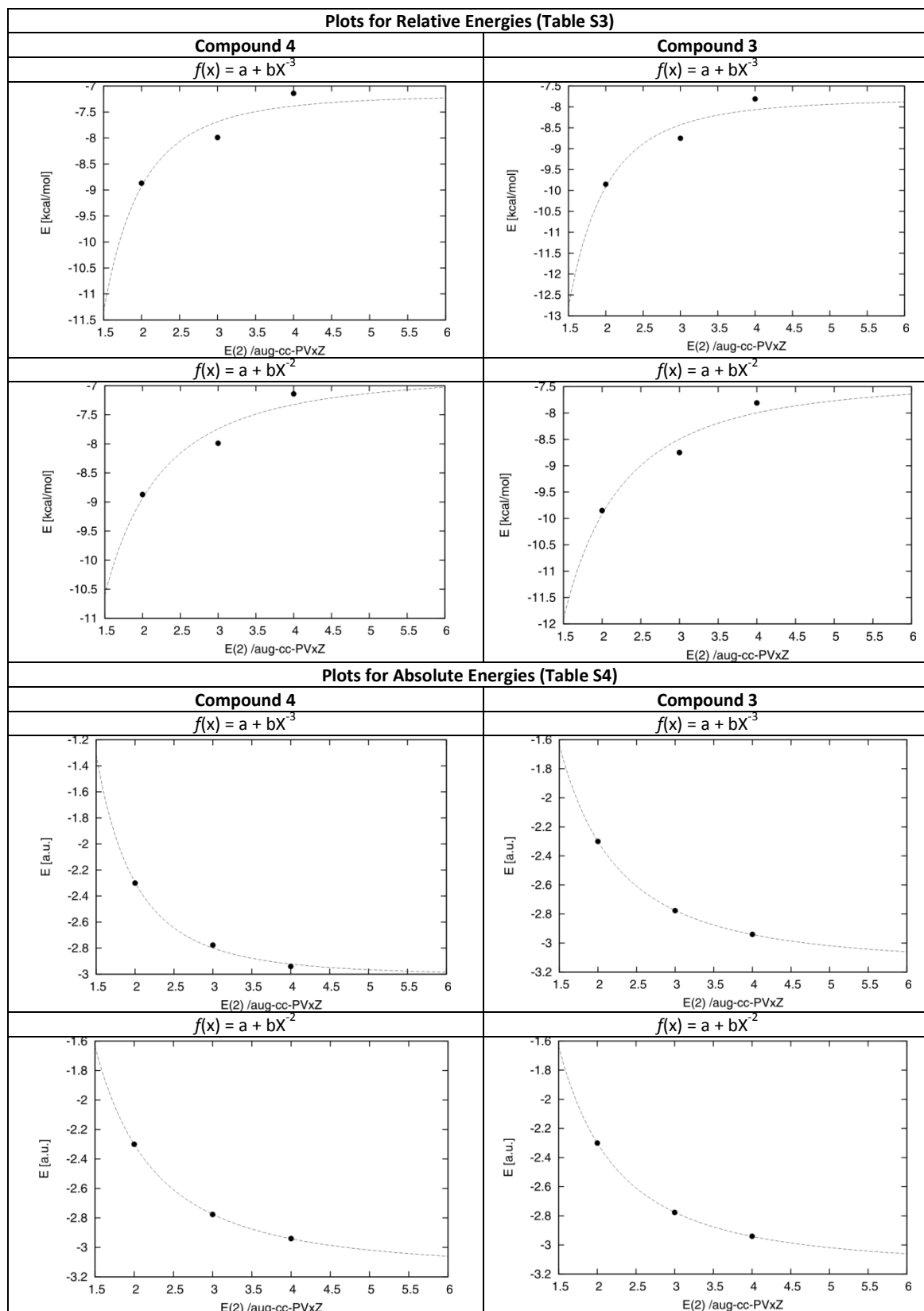**Figure S1:** Plots of equations $E^{(2)}$/CBS = a + bX^{-3} and $E^{(2)}$/CBS = a + bX^{-2} for X = 2, 3 and 4 (basis set aug-cc-pVXZ). $E^{(2)}$/CBS values used from Table S3 (relative energies) and Table S4 (absolute energies).

Table S6: Calculated ^{1}H isotropic shielding tensors and chemical shifts obtained at the BHandH/6-311+G(2d,p) level on B3LYP/def2-TZVP optimised geometries with BSSE corrections included.

	3		**4**		**3.C$_6$H$_6$**		**4.C$_6$H$_6$**			
	σ	δ	σ	δ	σ	δ	σ	δ	Δδ3	Δδ4
H$_{ax}$	27.31	4.90	30.22	1.99	28.42	3.79	30.93	1.28	-1.11	-0.71
H$_{eq}$ (down)	26.11	6.10	26.80	5.41	26.76	5.45	27.18	5.03	-0.65	-0.38
H$_{eq}$ (up)	---	---	28.92	3.29	---	---	29.30	2.91	---	-0.38

σ(TMS) = 32.21 ppm

Table S7: Calculated ^{1}H isotropic shielding tensors and chemical shifts obtained at the BHandH/6-311+G(2d,p) level on B3LYP-D3/def2-TZVP optimised geometries with BSSE corrections included.

	3		**4**		**3.C$_6$H$_6$**		**4.C$_6$H$_6$**			
	σ	δ	σ	δ	σ	δ	σ	δ	$\Delta\delta$**3**	$\Delta\delta$**4**
H$_{ax}$	27.51	3.74	30.25	1.00	28.39	2.86	30.94	0.31	-0.88	-0.69
H$_{eq}$ (down)	26.33	4.92	26.80	4.45	26.86	4.39	27.28	3.97	-0.53	-0.48
H$_{eq}$ (up)	---	---	28.93	2.32	---	---	29.48	1.77	---	-0.55

σ(TMS) = 31.25 ppm

Table S8: Calculated ^{1}H isotropic shielding tensors and chemical shifts obtained at the BHandH/6-311+G(2d,p) level on MP2/aug-cc-pVDZ optimised geometries.

	3		4		3.C_6H_6		4.C_6H_6			
	σ	δ	σ	δ	σ	δ	σ	δ	$\Delta\delta$**3**	$\Delta\delta$**4**
H_{ax}	27.24	4.01	29.94	1.31	28.08	3.17	30.60	0.65	-0.84	-0.66
H_{eq} **(down)**	26.08	5.17	26.53	4.72	26.58	4.67	27.00	4.25	-0.50	-0.47
H_{eq} **(up)**	---	---	28.59	2.66	---	---	29.12	2.13	---	-0.53

σ(TMS) = 31.25 ppm

Table S9: Calculated ^{1}H isotropic shielding tensors for "ghost" atoms obtained at the BHandH/6-311+G(2d,p) level on B3LYP/def2-TZVP optimised geometries with BSSE corrections included.

	3.C$_6$H$_6$	4.C$_6$H$_6$
	σ	σ
H$_{ax}$	1.18	0.88
H$_{eq}$ (down)	0.36	0.34
H$_{eq}$ (up)	---	0.28

a)   b)   c)
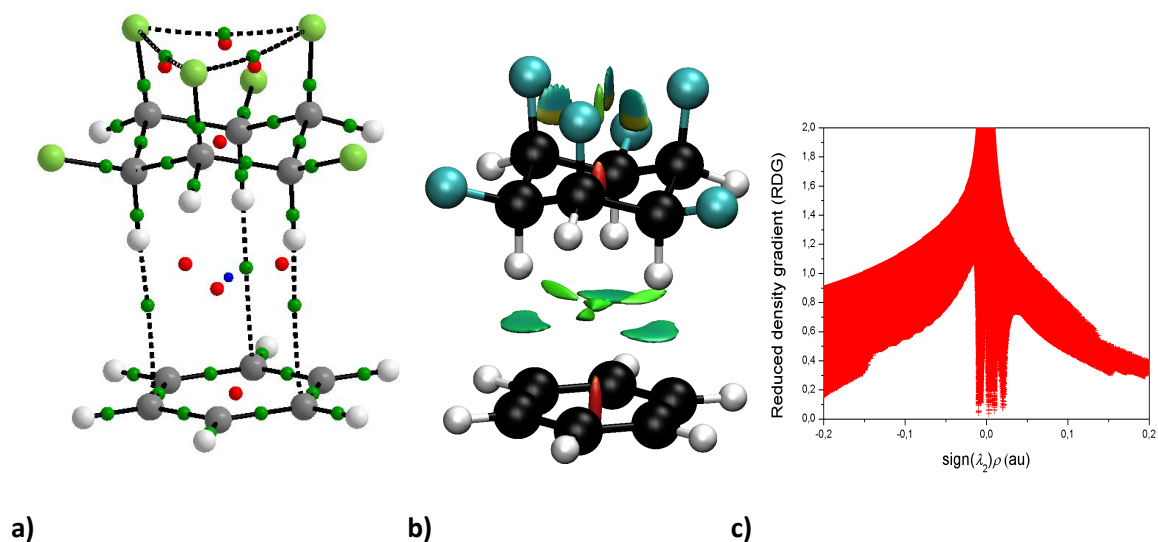
Figure S2: Results from topological analysis of the total electron density of **3**·C_6H_6 (MP2/aug-cc-pVDZ//MP2/aug-cc-pVDZ level): **a)** Molecular graph from Atoms-in-Molecules analysis; green: bond critical points (BCPs), red: ring critical points, blue: cage critical point. Key properties of the three BCPs connecting **3** to C_6H_6: ρ = 0.007, $\nabla^2\rho$ = +0.020, ellipticity=+0.393, K = -0.0006, V = −0.0038, G = +0.0044 (all in a.u.). **b)** NCI isosurfaces for **3**·C_6H_6 obtained with reduced density gradient (RDG) = 0.5 and blue-green-red color scale ranging from −0.02 a.u. < sign(λ_2)ρ(r) < +0.02 a.u. **c)** Graph of RDG versus sign(λ_2)ρ for **3**·C_6H_6. The regions between the axial H atoms of **3** and the closest C atoms of benzene are included in the downward peak at negative sign(λ_2)ρ, indicating weakly attractive interactions.
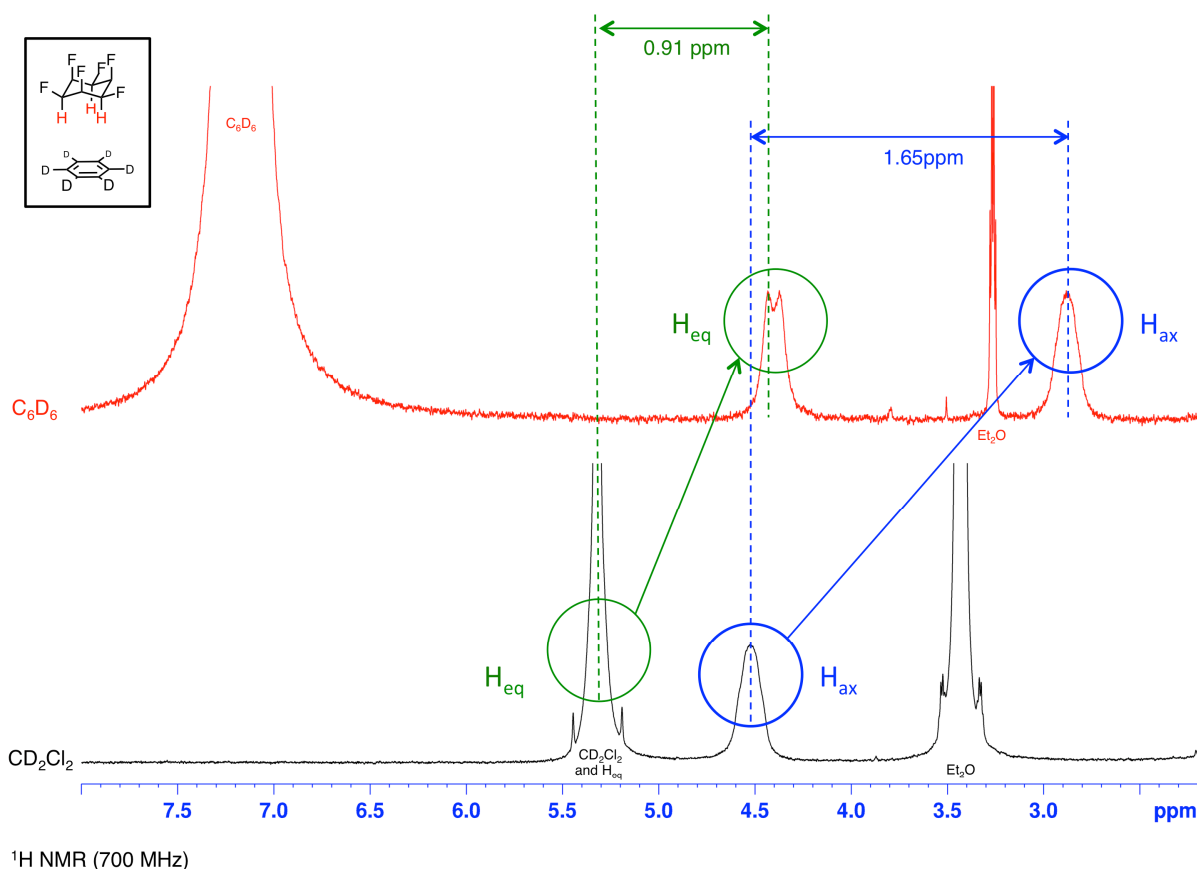
Figure S3: Experimental ^{1}H NMR spectra (700 MHz) of **3** in CD_2Cl_2 (bottom) and C_6D_6 (top) illustrating the upfield shifts of the signals on going into the aromatic solvent. An impurity of diethyl ether was present in the NMR samples.
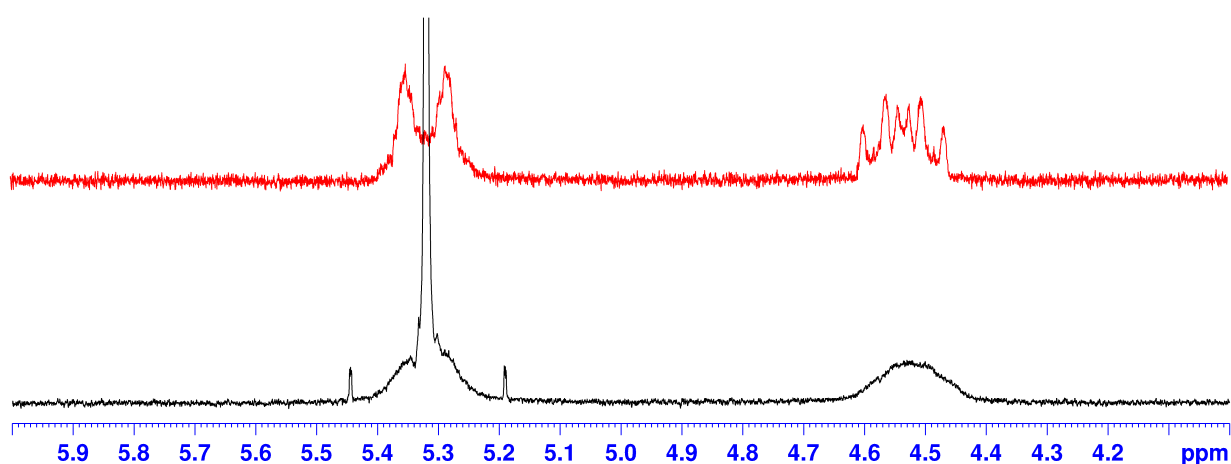

Figure S4: Experimental ^{1}H 1D gradient selective TOCSY NMR spectra (700 MHz) of **3** in CD_2Cl_2 (top), irradiated on the H_{ax} signal at 4.59 ppm and ^{1}H NMR of **3** in CD_2Cl_2 (bottom) illustrating the overlap of the H_{eq} protons of **3** with the residual CD_2Cl_2 solvent signal.